Available online at www.eccomasproceedia.org
Eccomas Proceedia UNCECOMP (2017) 576-587

ECCOMAS
Proceedia

UNCECOMP 2017
2nd ECCOMAS Thematic Conference on
Uncertainty Quantification in Computational Sciences and Engineering
M. Papadrakakis, V. Papadopoulos, G. Stefanou (eds.)
Rhodes Island, Greece, 15–17 June 2017

A COUPLED NUMERICAL AND LASER OPTICAL METHOD FOR ON-SITE CALIBRATION OF FLOW METERS

A. Weissenbrunner[1], A. Fiebach[1], M. Juling[1] and P.U. Thamsen[2]

[1]Physikalisch-Technische Bundesanstalt (PTB), Abbestr. 2-12, 10587 Berlin, Germany
[2]Technische Universität Berlin, Department of Fluid System Dynamics, Straße des 17. Juni 135, 10623 Berlin, Germany
andreas.weissenbrunner@ptb.de

Keywords: CFD, polynomial chaos, LDV, optimization, calibration, flow rate reconstruction, uncertainty quantification, pipe flow.

Abstract. *In this contribution it is intended to combine laser-optical measurements with numerical simulated flow profiles. This approach allows on-site calibration of installed flow meters and improves the accuracy of flow rate measurements under disturbed flow conditions. Since multiple pipe assemblies consecutively disturb the flow profiles, uncertain inflow conditions are considered in a polynomial chaos approach. Reynolds averaged Navier-Stokes equations (RANS) are solved to predict velocity profiles with inflow conditions from elbows out-of-plane with random distance to each other. Further, an optimization problem is solved in order to fit the simulated velocity profiles to the measurement data. The procedure is applied to different measurements from a test rig, for which the reference flow rate is known. The uncertainty of all measurements can be estimated very well. A reduction of the uncertainty by the procedure can however not always be assured, which is due to a lack of accuracy of the CFD simulations.*

Peer-review under responsibility of the organizing committee of UNCECOMP 2017.
doi: 10.7712/120217.5393.16913

1 INTRODUCTION

Elbow alignments are necessary in almost all pipe assemblies in industrial fields, especially in district heating systems. They introduce disturbance to the flow profiles that require a straight pipe length of several tenth diameters to be eliminated. Very often those parts are not sufficiently long to redevelop an ideal profile. Thus, flow rate measurements with ideal flow conditions are not possible. It is well known that many flow meters react sensitively to disturbed flow profiles, as they are usually calibrated under ideal conditions on test rigs. This has been demonstrated in numerous publications, for example see [1, 4, 7, 17, 9, 10, 14, 15]. The induced errors for large heat meters tested in district heating pipelines are typically higher than 3 % and could reach more then 20 %, see [3]. To determine these errors, an in-situ calibration technique with Laser Doppler Velocimetry (LDV) was developed in [12]. The technique enables to measure point wise the axial fluid velocity on a diametrical path through an inserted contour fitting window. Under the assumption of rotationally symmetric flow profiles the integral over the path gives the flow rate. In disturbed flow conditions the uncertainty is highly increased and depends on the exact shape of the flow profile at the measurement cross section, which is generally unknown. Therefore the idea is to simulate the velocity profile at the measurement cross section and combine the result with LDV measurements.

In cooperation with TU Berlin, ILA GmbH and Optolution Messtechnik GmbH the project "EnEff:Wärme: On-site calibration of flow meters in district heating" [2] was initiated. The goal is to develop a method which permits on-site calibration of installed flow meters in non ideal installation conditions.

Pipes of district heating systems are characterized by large diameters and high temperatures, which leads to high Reynolds number flows. Therefore, Reynolds Averaged Navier Stokes (RANS) Models are used to predict the flow profiles at the measurement cross sections. In this paper combinations of elbows out-of-plane with different distance to each other are considered as pipe assemblies. LDV Measurements with 4 different setups were conducted. For the simulations the distance of the elbows is considered as random in a non-intrusive polynomial chaos study. To combine measurement and simulation the uncertainty of a single path measurement is predicted with CFD simulations. To further improve uncertainties a minimization problem is formulated for which the distance and additionally the path angle are varied in order to fit the CFD profiles to the LDV.

In Section 2 the experimental setup is described and the measured velocity distributions are shown. In Section 3 the numerical setup is described, the expectation value and the standard deviation of the velocity profile are compared to the measurements. In Section 4 the CFD results are used to estimate and reduce the uncertainty of the flow rate prediction. The results for all measurements are displayed and discussed. The last Section concludes the paper.

2 EXPERIMENTAL SETUP

The most influencing distortions in pipe flow profiles arise from bended pipes out-of-plane. They cause asymmetric and swirling profiles which decay only slowly. Most studied out-of-plane configurations consider two elbows closely coupled with an ideal inlet profile [8, 11, 9, 6]. In industrial pipe assemblies this is not the case. In an earlier work [15] it was shown that upstream pipe elbows with different distances cause diverse flow profiles. Here a combination of three closely coupled bends is studied with preliminary distortion.

The inner pipe diameter D is 53.6 mm, whereas the curvature radius R_c of the 90° bends, according to the pipe center line, denotes 2.35 D. Compared to most other studied bends found in literature [11, 9, 5, 8] this is a relatively large curvature. Between each of the three closely coupled bends a straight pipe is mounted with a length of 3 D. Two assemblies of identical mirrored triple bends with varying distance to each other are installed before the measurement section, see Figure 1 left. Four experimental setups were conducted with intermediate distances 5, 10, 20 and 50 D. These measurements are referred as Measurement 1, 2, 3 and 4. The distance of the measurement section behind the last bend is fixed to 6 D.

To measure the velocity in the cross section a laser Doppler velocimeter (LDV) is used. LDV uses the Doppler shift of laser light, that is scattered by small particles within the fluid, to determine the velocity of the particles and hence the velocity of the fluid within a small measuring volume. The measuring volume is positioned on a Grid consisting of 49 diametrical and 10 angular locations, see Figure 1 right. The measurements were conducted on a test rig at the department of fluid system dynamics of the TU Berlin[1]. The test rig contains plastic pipes with a very smooth surface. The fluid is water, for which the temperature and velocity were chosen to match a Reynolds number of about $3 \cdot 10^5$.

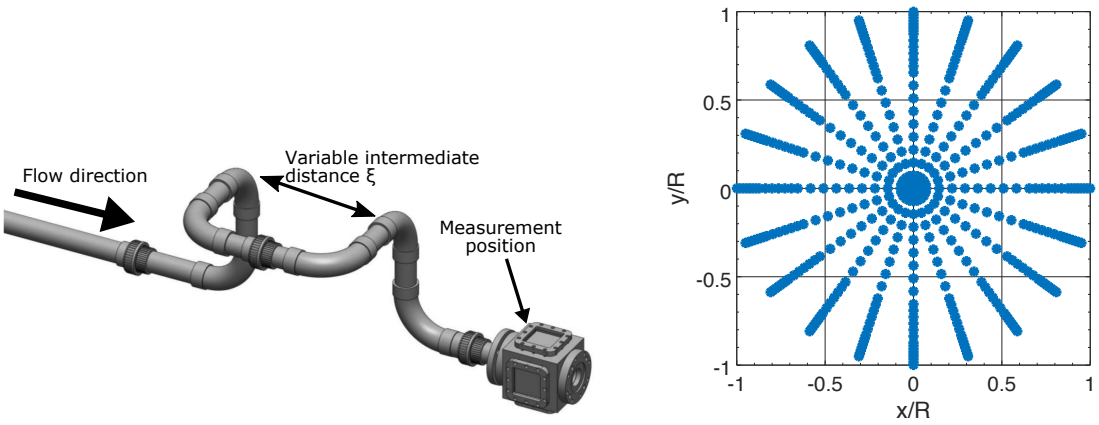

Figure 1: left: the six elbows with a window chamber at the measurement position, right: the measurement positions in the cross section.

Centrifugal forces cause the velocity profile behind a bend to be higher at the outer part. If another bend is closely coupled and rotated by 90 degrees in space, a swirling flow is generated. This causes the axial velocity distribution in a cross section to form a sickle shape. The three closely coupled elbows, which are considered here, cause similar effects. This can be observed in the measured velocity profiles in Figure 2. For different intermediate distances ξ of the two elbow packages the shape of the sickle as well as the azimuthal position are varying. The broadness of the sickle is decreasing for increasing intermediate distance. The azimuthal position of the sickle is located on the right hand side and varies by about 45°.

[1]Measurement data obtained by P. Kretschmer and A. Swienty

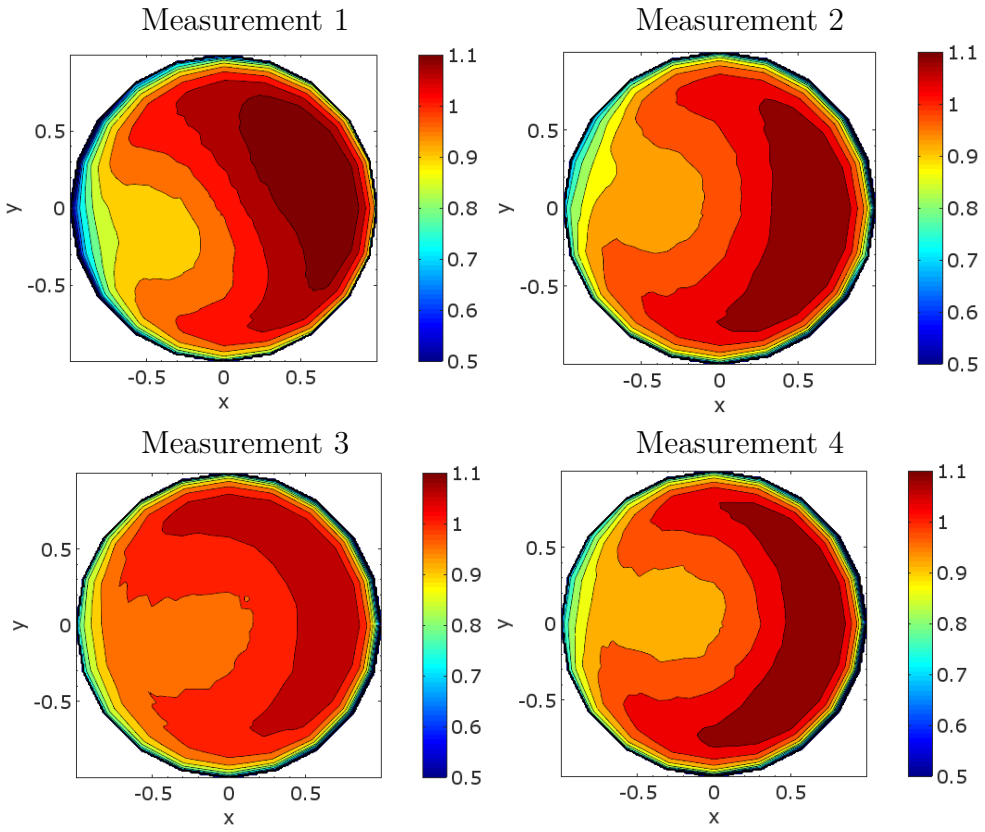

Figure 2: Normalized axial Velocity distribution u_z/u_{vol} 6 D downstream of the elbow combination. From the left top to right bottom: LDV measurements with intermediate distance 5, 10, 20 and 50 D.

3 NUMERICAL SETUP

The geometry of the experimental set up is reconstructed in a CAD model and spatially discretized with a hexahedral grid consisting of about 3.8 million elements, see Figure 3. To sufficiently resolve the wall layer the dimensionless wall distance y^+ is chosen to be close to 1. To ensure mesh independence a second Grid with 11 million elements was generated. The results with both grids exhibit only marginal differences. Hence, the coarse grid is sufficient. The solution of the governing Navier-Stokes equations is numerically expensive and for high Reynolds numbers not feasible. Hence a turbulence model is needed. Here the eddy viscosity Reynolds Averaged Navier-Stokes (RANS) k-ω model [16] is chosen. Due to the smooth pipe surface of the test rig pipes, no-slip boundary conditions on the walls and a zero-gradient condition at the outlet are chosen. At the inlet, a fully developed profile from an earlier simulation with associated turbulence data is used as a natural inflow boundary condition. The length of the straight pipe downstream of the elbows is 65 D. In a non intrusive polynomial chaos approach the distance of the preliminary group of three elbows is chosen as random. It is considered to be uniformly distributed between 4 and 60 D. Therefore all four measurement setups are included in the probability space. 20 sample positions are chosen for the polynomial chaos approach according to the nodes of the Gauß-Legendre quadrature. The commercial solver ANSYS CFX is used for the CFD calculations. The normalized axial velocity profile resulting from a simulation with ideal

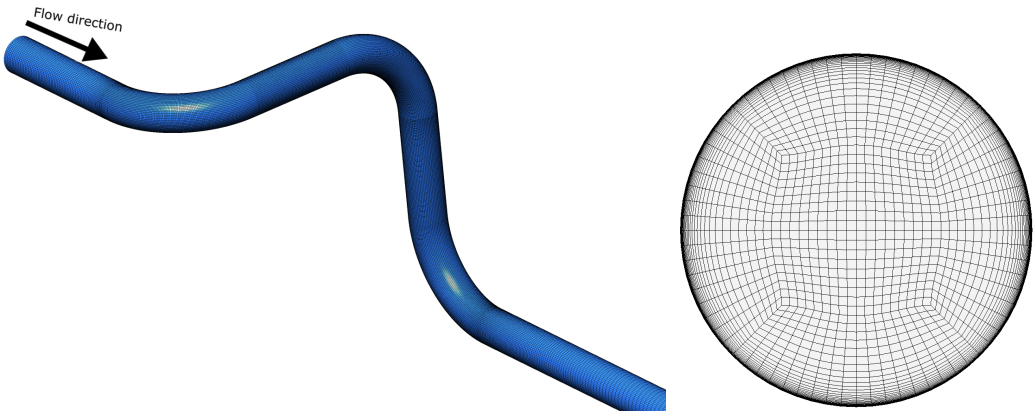

Figure 3: The grid of the triple elbow (left) and the inlet section of the simulation domain (right).

inflow conditions is shown in Figure 4 left. The expected axial flow profile, calculated with random intermediate distance and the associated relative standard deviation is shown in Figure 4. Similar to the measurements, shown in Figure 2, the position of the sickle is located on the right-hand side, but is more elongated than in the measurements. The standard deviation exhibits values of up to 10 % relative to the mean velocity u_{vol}. The lowest values are located on the lower right-hand side and form sickle shape. The highest values can be observed on the right and left side bordering the sickle shape.

4 COMBINATION OF CFD AND LDV

In the following laser optical and numerical methods are combined in order to firstly estimate and secondly reduce the uncertainty of the flow rate calculation. The volume

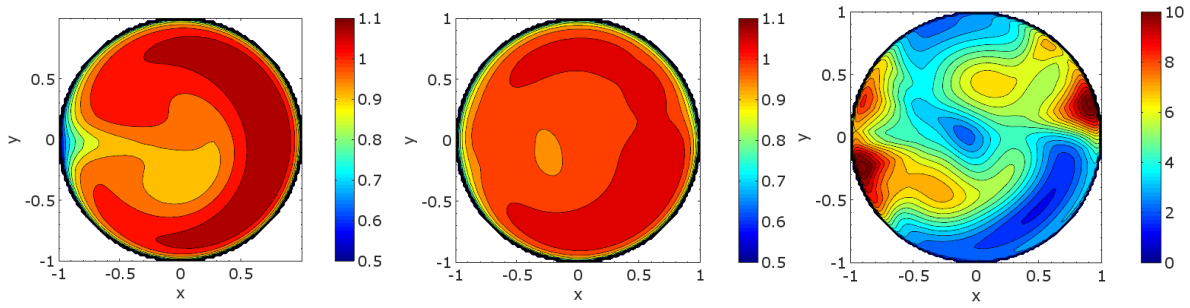

Figure 4: Simulated normalized axial Velocity distribution u_z/u_{vol} 6 D downstream of the triple elbow. With fully developed inflow conditions (left), expected profile (middle) and its standard deviation in % (right), from a polynomial chaos calculation.

flow rate from a single path LDV measurement is calculated by

$$Q = \pi \int_{-R}^{R} u_z(\varphi_p, r)\,|r|\,dr\,. \tag{1}$$

In case of a rotationally symmetric profile this leads to the exact value. However, for non symmetric profiles this leads to errors. In a first step the error range of the measurements is estimated by using CFD simulations. Note, that for all further calculations the reference flow rate Q_{ref} is defined by the mean value of the integrated LDV measurements. Due to reflections and other measurement inherit uncertainties, the values deviate slightly to the reference Meter on the test rig, but are neglected here.

4.1 Uncertainty estimation of the flow rate

The simulation result of the flow downstream the three elbows with fully developed inflow condition from Figure 4 is considered and the angle φ_p is set as random. This has been identified as a good approach in earlier research [15]. The error is defined as $(Q_p - Q_{ref})/Q_{ref} * 100$, where Q_p denotes the flow rate calculated with a diametrical path. When discretization errors are neglected, the resulting expected error must vanish, due to its definition (1). The results are shown in Figure 5. The standard deviation closely behind the bend outlet is up to 4 % and decreases until about 5 D to about 1.5 % and increases again until 20 D. From there on it slowly decreases and is still 2 % after 50 diameters of straight pipe, compare the red error bars. The blue error bars denote the maximum deviations that occur in the particular cross section. They exhibit a similar behavior with increasing distance to the elbows. The amplitudes of the negative deviations are higher and can lead to more than -8 % directly behind the bend and about -6 % in 20 D distance. The measurements are located in 6 D, which is in the area where the errors are expected to be the lowest. The evaluation of the standard deviation of the measurements (black) is with 1.2 % slightly lower than those predicted by the simulations. Also, the maximum and minimum deviations (green) are in the predicted scope.

4.2 Reduction of the flow rate uncertainty

In the next step a procedure is derived, that allows to reduce uncertainties of the flow rate calculation shown in Figure 5. Therefore, an optimization procedure is proposed in this section. As a measure for the difference $\varepsilon = u_s(r) - u_m(r)$ between the measured and

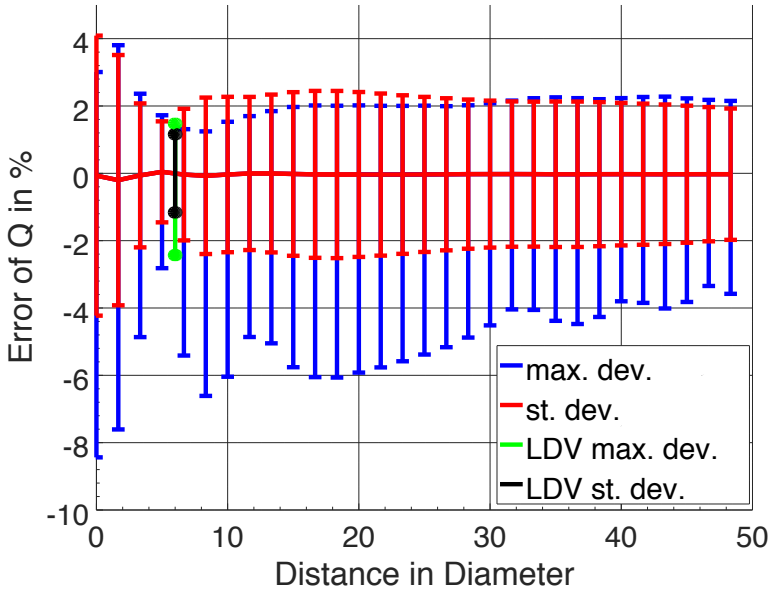

Figure 5: Error estimation of a single diametrical LDV-Measurement with CFD with random angular position of the evaluated path, over the distance to the bend outlet, blue: maximum and minimum deviation, red: standard deviation from the CFD simulation, green and black: maximum/minimum and standard deviations from measurements.

simulated velocity profile along a diametrical path, the L^2-norm in polar coordinates

$$\|\epsilon\| = \left(\int_{-R}^{R} \int_{0}^{\pi} \varepsilon^2 \, |r| \, d\varphi \, dr \right)^{\frac{1}{2}} = \pi \left(\int_{-R}^{R} \varepsilon^2 \, |r| \, dr \right)^{\frac{1}{2}} \tag{2}$$

is considered, whereas R denotes the maximum radius r of the pipe cross section. The flow rate is the quantity of interest and therefore unknown. However in the simulations the flow rate must be (implicitly) set in the boundary inlet condition. To conduct the simulations the flow rate Q_s is estimated. Those estimations can result from the integral of a single path measurement or an installed flow meter. However the flow rate in the simulation Q_s is defective. To compensate these errors a constant factor F is introduced, which multiplies the simulated velocity profile to best fit the measured velocity profile, i.e. $Q_c = FQ_s$. Additionally the velocity distribution of the simulation is depending on the inlet condition, e.g. the distance to the preliminary bends $\xi \in \Omega = [4, 64]\, D$. The angle φ_p of the diametrical path can also be varied. This results in the non-linear, non convex optimization problem

$$T = \left\| F\tilde{u}_s \left(\xi, \varphi_p, r\right) - u_m \left(r\right) \right\|, \min_{\forall \xi \in \Omega, \varphi \in [0, 2\pi], F \in \mathbf{R}^+} T. \tag{3}$$

The velocity profile for a certain inlet condition $\tilde{u}_s$ is assembled by a sum over all modes for a certain radius and angle $\hat{u}_i(\xi, \varphi_p, r)$ multiplied with the orthogonal polynomials $P_i(\xi)$

$$\tilde{u}_s \left(\xi, r\right) = \sum_{i}^{N_m} \hat{u}_i \left(r\right) P_i \left(\xi\right). \tag{4}$$

From the optimization criteria $\frac{\partial T}{\partial F} = 0$ the factor F can be determined by

$$F(\xi, \varphi_p) = \frac{\int_{-R}^{R} u_m(r)\tilde{u}_s(\xi, \varphi_p, r)\,|r|\,dr}{\int_{-R}^{R} \tilde{u}_s^2(\xi, \varphi_p, r)\,|r|\,dr}. \tag{5}$$

The derivatives of T for the other variables ξ and φ_p can not be calculated directly and would lead to a new minimization problem, which is not considered here. In order to simplify the calculation the optimal factor $F(\xi, \varphi_p)$ is inserted into the target function 3. The resulting optimization problem is reduced by one dimension

$$T = \left\| F(\xi, \varphi_p)\tilde{u}_p(\xi, \varphi_p, r) - u_m(r) \right\|, \min_{\forall \xi \in \Omega, \varphi \in [0, 2\pi]} T. \tag{6}$$

To solve the minimization problem (6) the downhill simplex algorithm according to Nelder and Mead [13] is used. To distinguish the global minimum the algorithm is started with different initial conditions. All Integrals are numerically solved by a trapezoidal rule.

4.3 Results

The procedure is applied to Measurement 1-4 in Figure 2. Different variations, e.g. of the angle φ_p and the distance between the elbows ξ were conducted. The variation of the path angle shows the best results. The errors for all measurements are shown in Figure 6. Each path is treated as a single LDV measurement. The errors are in percent relative to the mean value of all path integrations according to (1). The errors of the integration of each path is shown in blue circles connected with lines. All measurements show a periodic behavior with amplitudes of about 2 %. Applied to each particular measurement the proposed procedure behaves differently. For Measurement 3 the error decreases for each path. The mean error of the combined procedure, depicted as red dashed line, is staying around zero. For Measurement 2 and 4 the error for about half of the paths is decreased. For the other half the error slightly increases. The mean value in both cases is increasing to about 1 %. For Measurement 1, in which the distance between the two elbow conjunctions is 5 D, the combined procedure lowers the error only in one path. In every other path the error is increased, the mean error is about 3 %. The value of the target function (6) is represented by red error bars. It is proposed to be a measure for the uncertainty for a single path measurement. It can be observed that in almost all cases the error bar covers the zero error line. Nonetheless, the size of the error bars do not always correspond to the present error and seem to be too large. To assess the performance of the combined method the standard deviation of the error over the paths is compared in Figure 7. The standard deviation of the errors that are calculated solely by integration of the LDV profiles is depicted in blue and for the combined algorithm in red. While the standard deviation for Measurement 2, 3, and 4 is drastically reduced, it is slightly enhanced for Measurment 1. The yellow bars represent the value of the expected error for the combined procedure. It is added to the standard deviation as an additional uncertainty. For Measurements 1 and 2 the uncertainty is enhanced by the combined algorithm. For Measurement 3 and 4 a reduction of the uncertainty is still achieved by the combined procedure.

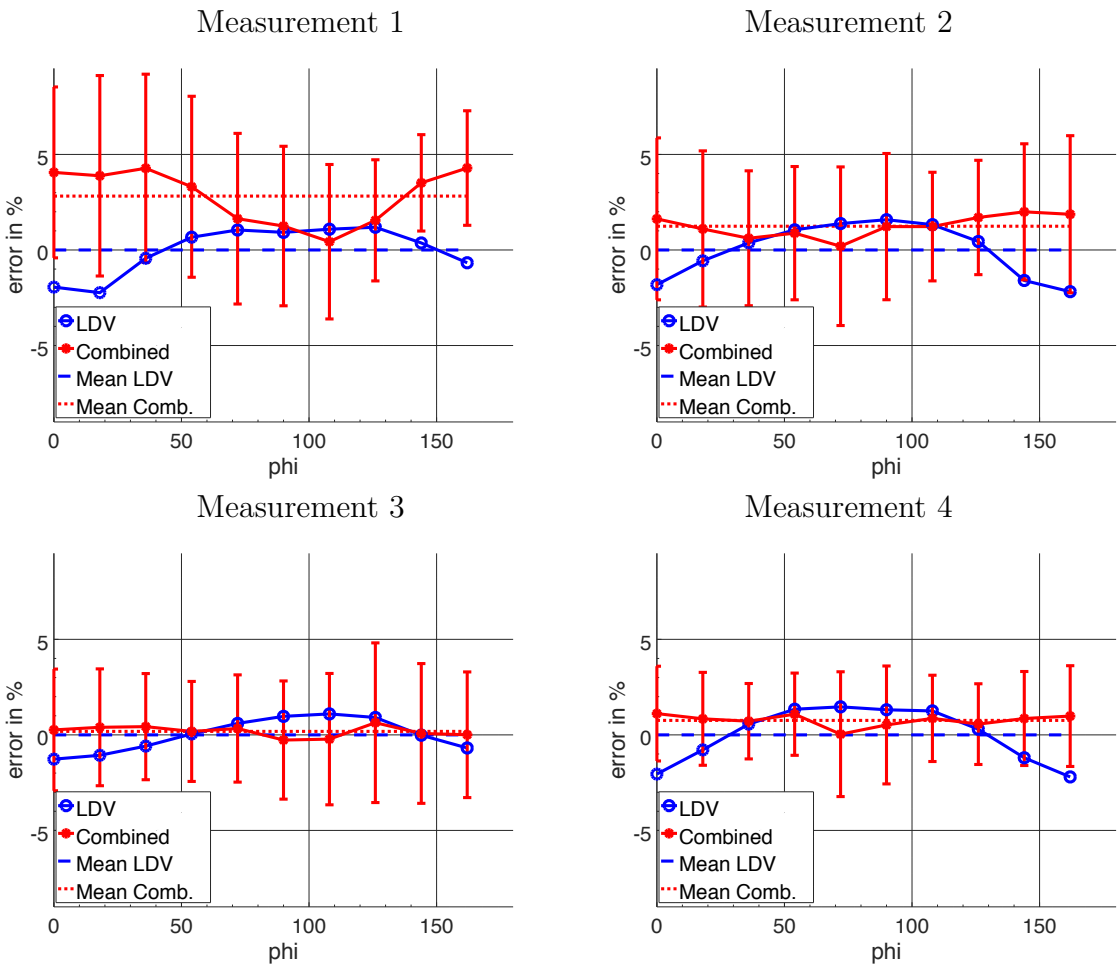

Figure 6: Normalized axial Velocity distribution u_z/u_b 6 D downstream of the triple elbow combination with different distances to the preliminary elbows. From the left top to right bottom: 5, 10, 20 and 50 D, corresponding to Measurement 1-4 in Figure 2.

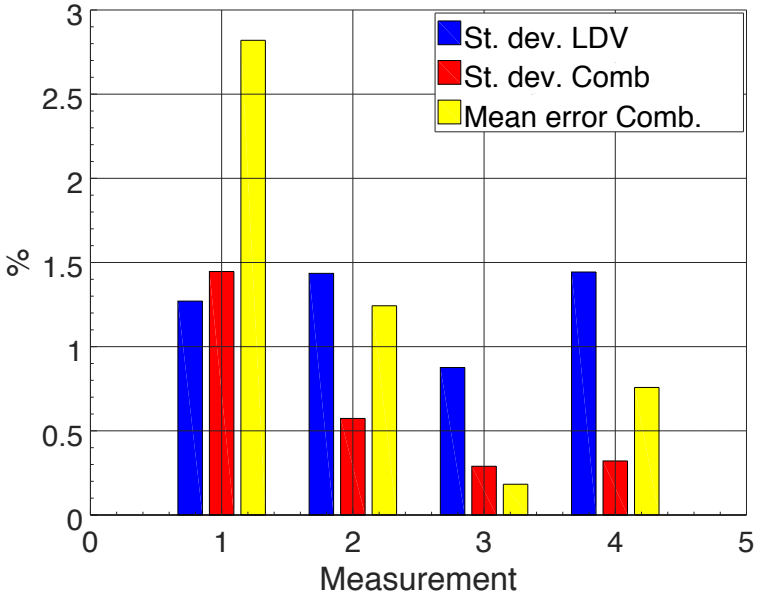

Figure 7: Standard deviation of the flow rate calculation for Measurement 1-4. With LDV (blue) and the combined procedure (red). The mean error of the combined procedure is shown in yellow.

5 CONCLUSIONS

In this paper systematic errors of single path laser Doppler velocimetry (LDV) measurements in asymmetric swirling flows behind several elbows out-of-plane are investigated. To do so, simulations with Reynolds averaged Navier-Stokes equations (RANS) are performed. Firstly it is demonstrated, that the uncertainty of the calculated flow rate due to the integration of a single diametrical LDV path can be well estimated with computational fluid dynamics. Therefore, the angle is set as random and the standard deviation is used as a measure for the uncertainty. Secondly, a method is derived to fit a simulation result to a measurement by solving an optimization problem. Due to the adapted simulation a factor is introduced that estimates the flow rate, while the value of the target function is proposed as a measure for the uncertainty of the coupled numerical and laser optical procedure. Four LDV measurments were studied.

For two cases the uncertainty does not change much. Due to the lack of accuracy of the RANS turbulence models for swirling flows the uncertainty for one case is increased. It is expected that with advanced turbulence modeling the uncertainties will be decreased. This is confirmed for one case for which it leads to a significant reduction of the measurement uncertainty. This shows the potential of the combination of CFD and LDV applied to measurements under disturbed flow conditions.

ACKNOWLEDGMENT

A. Weissenbrunner was supported by the Federal Ministry for Economic Affairs and Energy within the EnEff:Wärme project ”On-site calibration of flow meters in district heating”. A. Fiebach was supported by the European Commission and EURAMET within the EMRP NEW-04 project ”Novel mathematical and statistical approaches to uncertainty evaluation”. The authors would like to thank all members of the EnEff-project for their assistance, especially A. Swienty and P. Kretschmer for providing the measurement data.

Supported by:

on the basis of a decision
by the German Bundestag

REFERENCES

[1] Carl Carlander and Jerker Delsing. Installation effects on an ultrasonic flow meter. In *FLOMEKO*, pages 149–154, 1998.

[2] German Federal Ministry for Economic Affairs and Energy (BMWi). On-site calibration of flow meters in district heating, 2013.

[3] Peter Guntermann, Jürgen Rose, Thomas Lederer, Michael Dues, Ulrich Müller, and Andreas Duckwe. In situ calibration of heat meters in operation. *EuroHeat&Power*, 8:46–49, 2011.

[4] J. Halttunen. Installation effects on ultrasonic and electromagnetic flowmeters: a model-based approach. *Flow Measurement and Instrumentation*, 1:287–292, 1990.

[5] Leo H. O. Hellström, Metodi B. Zlatinov, Guangjun Cao, and Alexander J. Smits. Turbulent pipe flow downstream of a bend. *Journal of Fluid Mechanics*, 735:R7 1–12, 2013.

[6] J. E. Heritage. The performance of transit time ultrasonic flowmeters under good and distrurbed flow conditions. *Flow Measurement and Instrumentation*, 1(1):24–30, 1989.

[7] P.E. Eric Kelner. Flow meter installation effects. In *American School of Gas Measurement Technology*, 2007.

[8] G. E. Mattingly and T. T. Yeh. Flowmeter installation effects due to several elbow configurations. In *North American Fluid Flow Measurement Conference (NAFFMC)*, 1990.

[9] Wolfgang Merzkirch, Klaus Gersten, Franz Peters, Venkatesa Vasanta Ram, Ernst von Lavante, and Volder Hans. *Fluid Mechanics of Flow Metering*. Springer, 2005.

[10] B. Mickan, G. Wendt, R. Kramer, and D. Dopheide. Systematic investigation of pipe flows and installation effects using laser doppler anemometry – part ii. the effect of disturbed flow profiles on turbine gas meters – a describing empirical model. *Flow Meas. Instrum.*, 7:151–160, 1996.

[11] Bodo Mickan. *Systematische Analyse von Installationseffekten sowie der Effizienz von Strömungsgleichrichtern in der Großgasmengenmessung*. PhD thesis, 1999.

[12] Ulrich Müller, Franz Adunka, Michael Dues, Peter Guntermann, Jürgen Rose, and Thomas Lederer. Möglichkeiten zur Vor-Ort-Überprüfung von großen Durchflusssensoren. *EuroHeat&Power*, 7-8:52–55, 2011.

[13] J. A. Nelder and R. Mead. A simplex method for function minimization. *Computer Journal*, 7:308–313, 1965.

[14] Karsten Tawackolian. *Fluiddynamische Auswirkungen auf die Messabweichung von Ultraschall-Durchflussmessgeräten*. PhD thesis, TU-Berlin, 2013.

[15] A. Weissenbrunner, A. Fiebach, S. Schmelter, M. Bär, P.U. Thamsen, and T. Lederer. Simulation-based determination of systematic errors of flow meters due to uncertain inflow conditions. *Flow Measurement and Instrumentation*, 52:25–39, dec 2016.

[16] D.C. Wilcox. Multiscale model for turbulent flows. In *AIAA 24th Aerospace Sciences Meeting. American Institute of Aeronautics and Astronautics*, 1986.

[17] T. T. Yeh and G. E. Mattingly. Flowmeter installation effects due to a generic header. Technical Note 1419, National Institute of Standards and Technology, 1996.